Protein Science (1996), 5:1898–1906. Cambridge University Press. Printed in the USA.

A dynamic bundle of four adjacent hydrophobic segments in the denatured state of staphylococcal nuclease

YI WANG AND DAVID SHORTLE

Department of Biological Chemistry, The Johns Hopkins University School of Medicine, Baltimore, Maryland 21205

(RECEIVED May 16, 1996; ACCEPTED June 28, 1996)

Abstract

In an earlier study of the denatured state of staphylococcal nuclease (Wang Y, Shortle D, 1995, *Biochemistry 34*:15895–15905), we reported evidence of a three-strand antiparallel beta sheet that persists at high urea concentrations and is stabilized by a local "non-native" interaction with four large hydrophobic residues. Because the amide proton resonances for all of the involved residues are severely broadened, this unusual structure is not amenable to conventional NMR analysis and must be studied by indirect methods. In this report, we present data that confirm the important role of interactions involving four hydrophobic residues (Leu 36, Leu 37, Leu 38, and Val 39) in stabilizing the structure formed by the chain segments corresponding to β1-β2-β3-h, interactions that are not present in the native state. Glycine substitutions for each of these large hydrophobic residues destabilizes or disrupts this beta structure, as assessed by H_N line sharpening and changes in the CD spectrum. The ^{13}C resonances of the carbonyl carbon for several of the residues in this structure indicate conformational dynamics that respond in a complex way to addition of urea or changes in sequence. Studies of hydrogen exchange kinetics in a closely related variant of staphylococcal nuclease demonstrate the absence of the stable hydrogen bonding between the strands expected for a native-like three-strand beta sheet. Instead, the data are more consistent with the three beta strand segments plus the four adjacent hydrophobic residues forming a dynamic, aligned array or bundle held together by hydrophobic interactions.

Keywords: folding intermediates; hydrogen exchange; hydrophobic interactions; non-native structure

Kinetic studies of protein folding suggest that there is an initial, rapid collapse of the unfolded polypeptide chain to form a hydrophobic core, followed by a series of slower steps that end when the native state is reached (Miranker & Dobson, 1996). Some models of the folding process propose that secondary structure formation precedes the initial collapse, whereas others suggest the collapse of the chain to a compact state may precede formation of secondary structure. Because of the difficulty of analyzing structure on time scales of a few milliseconds or less, much uncertainty surrounds these earliest events in folding.

Yet an argument can be made that these very early events may involve the most important steps in the folding process because they probably establish the global topology of the folded conformation. Because the number of possible conformations is reduced astronomically by these initial events (Dill, 1985), an understanding of the rules governing the energetics of chain–chain interactions taking place before or during the initial collapse is likely to be of great use for predicting protein structure from amino acid sequence.

As an alternative to tracking the buildup of structure as a function of time, our laboratory has been analyzing the folding of staphylococcal nuclease as a series of equilibrium steps in which conditions are made progressively more favorable for structure formation (Wang et al., 1995; Shortle, 1996; Shortle et al., 1996). A large fragment of staphylococcal nuclease missing six structural residues at the amino terminus and one structural residue at the carboxy terminus has been studied extensively as a model of the denatured state under physiologic conditions (Alexandrescu et al., 1994; Alexandrescu & Shortle, 1994; Wang & Shortle, 1995). Perhaps the most surprising observation has been that, at high urea concentrations, a segment of nuclease in the denatured state appears to form a three-strand antiparallel beta sheet (a beta meander), which is stabilized by a local, non-native interaction with four large hydrophobic residues (Wang & Shortle, 1995).

A model of this beta strand structure, shown in Figure 1, was proposed on the basis of the following NMR and CD data. (1) In the absence of urea, none of the H_N resonances were observed for the chain segment corresponding to residues 13–44, referred to here as the β1-β2-β3-h segment. Because ^1H-^{15}N correlation spectra were collected at pH 5.3 and 32 °C, conditions where the kinetics of hydrogen exchange are very slow (1–10 s^{-1}), we inferred

Reprint requests to: David Shortle, Department of Biological Chemistry, The Johns Hopkins University School of Medicine, Baltimore, Maryland 21205.

Abbreviations: HSQC, heteronuclear single quantum coherence; NTCB, 2-nitro-5-thiocyanatobenzoic acid; pdTp, 3',5' thymidine bisphosphate.

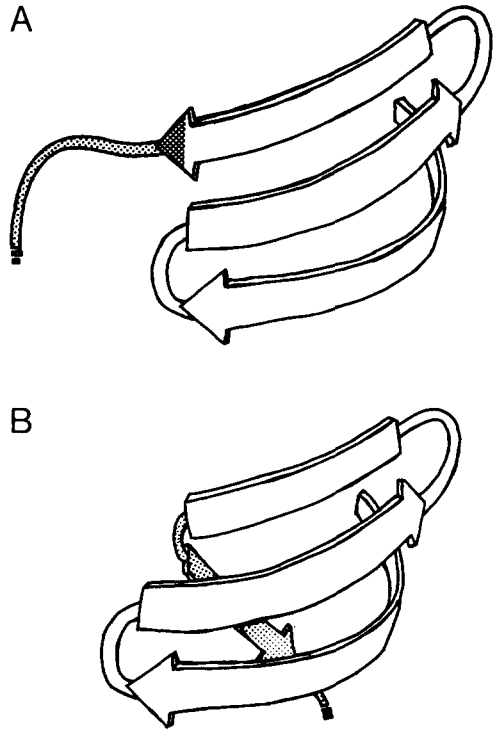

Fig. 1. Ribbon diagram showing the structure formed by the β1-β2-β3-h segment (residues 13–39). **A:** Native state of staphylococcal nuclease. **B:** Minimalist model of an unusual set of interactions in the denatured state (from Wang & Shortle, 1995). Cross-hatched segment corresponds to residues Leu 36, Leu 37, Leu 38, and Val 39.

that all of these residues must experience severe broadening from exchange between multiple conformations with different chemical shifts. Recent small angle X-ray scattering data on 1.5-mM solutions of Δ131Δ show no detectable aggregation, ruling out the possibility that this broadening arises from an intermolecular interaction involving the β1-β2-β3-h segment (M. Kataoka & D. Shortle, unpubl. obs.). (2) With increasing urea concentration, changes in the far-ultraviolet (UV) CD spectrum and the ^{1}H-^{15}N correlation spectrum indicated that beta-like structure is lost in concert with the appearance of all of the missing amide protons. (3) The ^{13}C carbonyl resonances of a number of residues in the β1-β2-β3-h segment were severely broadened and shifted upfield, suggesting the presence of an extended secondary structure.

In this report, we describe experimental data that strongly support the conclusions that interaction with hydrophobic residues Leu 36, Leu 37, Leu 38, and Val 39, which form no contacts with the three-strand antiparallel sheet (β1-β2-β3) in the native conformation, play an important role in this structure formed in the denatured state, and that there is no stable pairing between strand segments β1, β2, and β3 as would be expected for a native-like beta meander.

Results

Effects of mutations in the β1-β2-β3-h segment on the ^{1}H-^{15}N HSQC and CD spectra

Because of the severe broadening of the H_N resonances for the residues in the β1-β2-β3-h segment (T13 to V39) in the Δ131Δ model of the denatured state of staphylococcal nuclease (residues 1–3, 13–140), conventional NMR techniques provide little direct information on the structure formed by this segment. In the "minimalist" model consistent with the limited data available (Wang & Shortle, 1995; see Fig. 1), the h segment (L36–V39) is folded back to interact with the three-strand beta sheet on the basis of two lines of data: This interaction is inferred from the observation that the amide protons for L36, L37, L38, and V39 all disappear in concert with the amide protons of residues in β2-β3 on lowering the urea concentration below 6 M, suggesting that they participate in the same dynamic set of structures. In addition, the ^{13}C-carbonyl resonance of V39 and L36 (or L37) are severely broadened and shifted upfield, as are a number of hydrophobic residues in β1-β2-β3.

In order to test and refine the details of this model, indirect approaches must be applied, that is, methods that do not yield high-resolution information about molecular structure. Previous studies have shown that high urea or low pH reduce the stability or disrupt the β1-β2-β3-h structure, leading to a reduction or elimination of the severe line broadening and appearance of the amide protons in the NMR spectrum. Therefore, it was assumed that mutation of any residue that plays an essential role in stabilizing this structure should similarly sharpen the H_N resonances, or at least reduce the concentration of urea required for line sharpening.

To characterize the role of the four hydrophobic residues in the h segment following the β3 segment in stabilizing this structure, the effects of glycine substitutions on the NMR and CD spectra were characterized. Figure 2 shows the ^{1}H-^{15}N correlation spectra of Δ131Δ with the "wild-type" sequence (WT) and the Δ131Δ fragment containing the mutation L37G, with both spectra collected in the absence of urea. As is evident, a significant number of new peaks appear in Δ131Δ(L37G), all of which correspond to or are consistent with residues in the β1-β2-β3-h segment.

Similar spectra were collected for the Δ131Δ fragment with the single mutations V23G, F34G, L36G, L38G, V39G, and Y91G (a mutant outside the β1-β2-β3-h segment). In addition to spectra in the absence of urea, ^{1}H-^{15}N correlation spectra were obtained at several urea concentrations to assess semi-quantitatively what changes in stability or dynamic behavior had occurred. In addition, by comparison of ^{1}H and ^{15}N chemical shifts in 6 M urea, the amide peaks could be assigned unambiguously for these mutant fragments except for a few residues at ±1 and ±2 from the position of the glycine substitution. In Figure 3, the relative peak heights of several H_N from each of the four segments are tracked through the urea titrations. Mutant L37G has the most dramatic effect, causing all peaks to be observable in the absence of urea, with only small increases in peak intensity up to 2 M urea. All of the other mutations in the β1-β2-β3-h segment produce moderate to large effects on the urea titration, whereas three mutations outside this segment—Y91G, V74G, and L125G (the latter two are not shown)—exhibit the same behavior as WT. Because no significant changes in ^{1}H-^{15}N chemical shift were induced by the addition of increasing concentrations of urea, it seems unlikely that these mutations simply increase the rate of exchange between conformations without perturbing their structure and/or their relative populations.

The CD spectra of this same collection of mutant forms suggest a similar pattern of disruption of beta structure. As seen in Figure 4, the mutants with the most profound effect on the HSQC spectrum at 0 M urea also causes the largest reduction in the ellipticity at 215 nm. Although the NMR and CD data are difficult

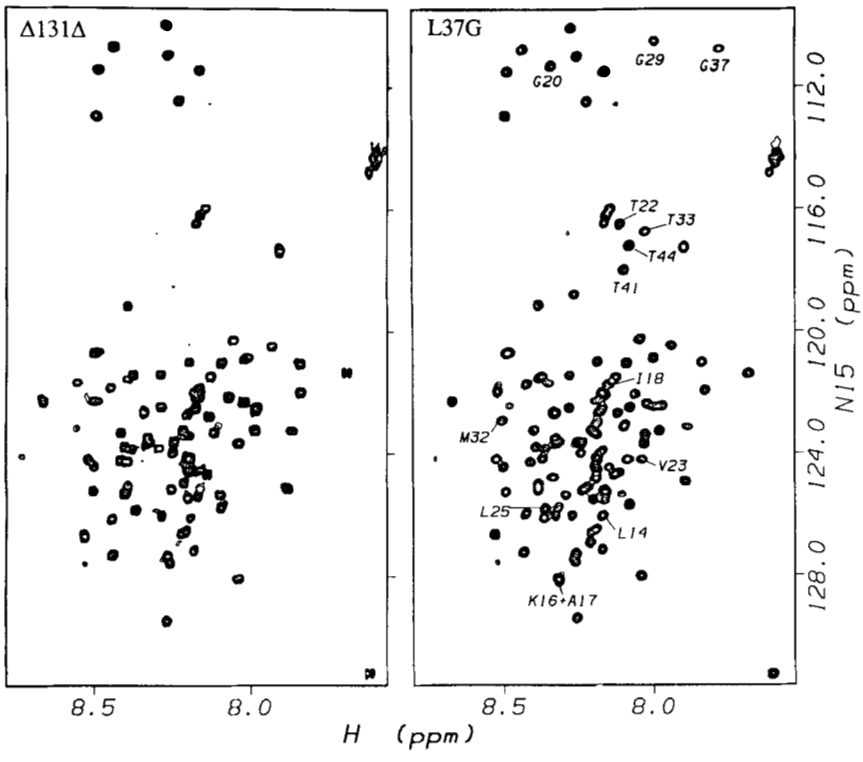

Fig. 2. ^{1}H-^{15}N correlation spectra of the Δ131Δ fragment of staphyloccal nuclease, pH 5.3, 32 °C. **A:** Wild-type sequence. **B:** L37G mutant. Labeled peaks are tentatively assigned on the basis of the Δ131Δ(WT) assignments obtained in 6 M urea (Wang & Shortle, 1995).

to compare quantitatively, it is clear that mutant effects on the CD spectrum are not as pronounced as those on the ^{1}H-^{15}N correlation spectrum. The largest mutant effect on the ellipticity (L37G) is roughly equivalent to the effect of 2 M urea on the spectrum of WT, namely a reduction in Θ_{215} by approximately half that seen in 6 M urea. However, in 2 M urea, none of the missing WT H_N are

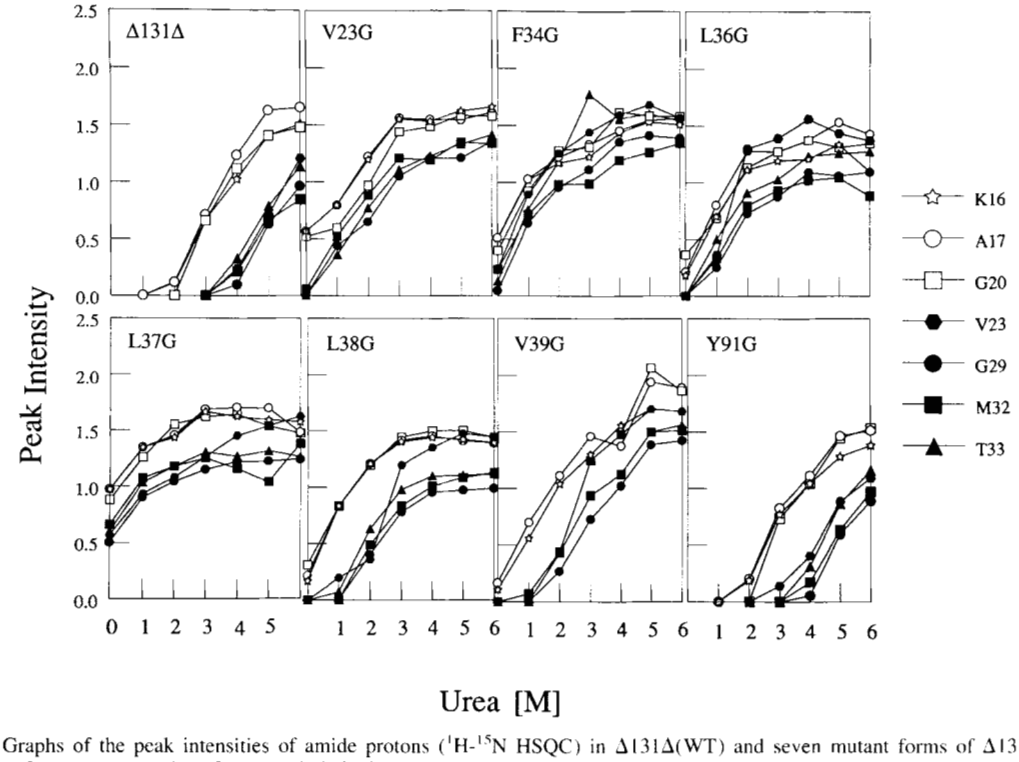

Fig. 3. Graphs of the peak intensities of amide protons (^{1}H-^{15}N HSQC) in Δ131Δ(WT) and seven mutant forms of Δ131Δ as a function of urea concentration. Open symbols indicate resonances from the β1 segment; solid symbols indicate resonances from the β2 and β3 segments.

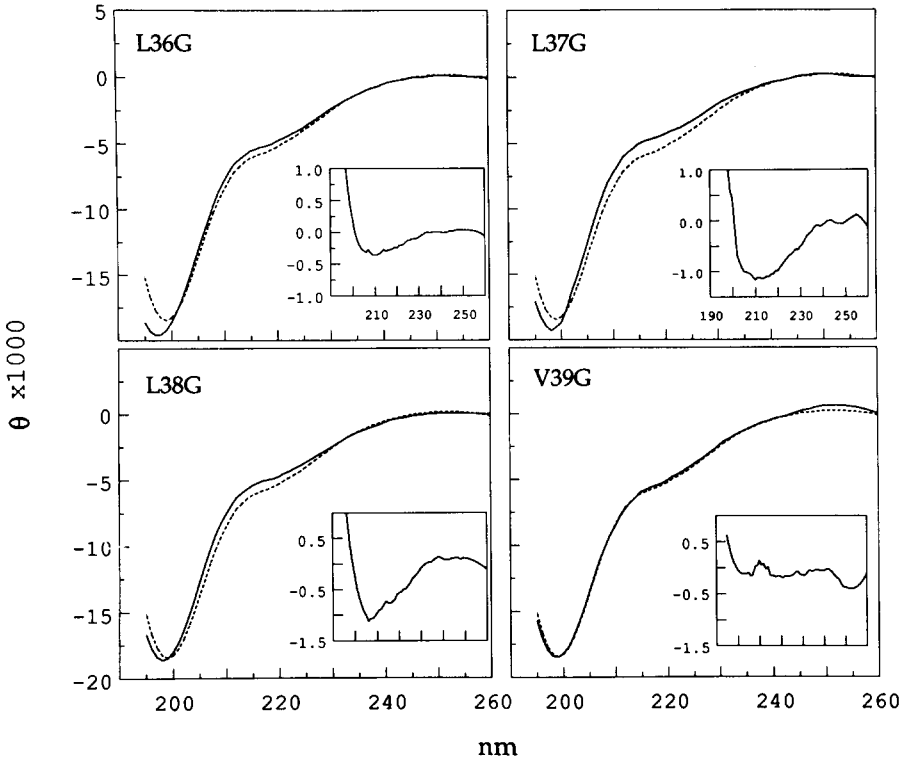

Fig. 4. CD spectra of four glycine substitution mutants in the h segment of Δ131Δ, pH 5.3, 32 °C. Solid line is the spectrum of the mutant protein, dashed line the spectrum of wild-type Δ131Δ. The difference spectra (WT − mutant) are shown in the insets. Ellipticity is expressed in deg cm^2 $dmol^{-1}$.

observable, whereas all of these resonances can be seen in the L37G mutant in the absence of urea. The most likely explanation for the smaller response of the CD spectrum to mutations than to urea is that this denaturant may be disrupting other beta-like structures within Δ131Δ, perhaps involving beta strands β4, β5, or β6. This conclusion is supported by CD data on the 1–44 fragment presented below.

^{13}C-carbonyl spectra of labeled Δ131Δ

By the incorporation of single amino acids (phenylalanine, methionine, valine, isoleucine, and leucine) with a unique ^{13}C label at the carbonyl position, the ^{13}C′ resonances of ten residues in the β1-β2-β3-h segment could be assigned (Wang & Shortle, 1995). All of these resonances were severely broadened and shifted upfield, consistent with exchange broadening involving a beta strand or extended conformation (Wishart et al., 1991; Wishart & Sikes, 1994). When these resonances are tracked as a function of urea concentration, several common features are observed (Fig. 5 shows only ^{13}C′-leucine and -methionine). For most resonances, the response to low concentrations of urea is an initial shift of the broad ^{13}C′ peak downfield toward a random coil chemical shift, followed at higher urea concentrations by a narrowing of the peak. The onset of line narrowing is often in the range of 2–3 M urea, which coincides with the appearance of the H_N resonances for residues in the β1 segment.

The L37G mutant form was also analyzed with this same set of single amino acid labels and direct-detect ^{13}C-carbonyl NMR (Fig. 5). No broadened peaks were observed for any of the five labels, and titration with urea led to no or only minor changes in chemical shifts. Thus, as with the amide protons, the behavior of the carbonyl resonances suggests that the L37G mutant has modified or disrupted the β1-β2-β3-h structure, not simply enhanced the rates of interconversion among alternate conformations with different chemical shifts.

To obtain additional secondary shifts for the ^{13}C-carbonyl resonances of other residues in Δ131Δ(L37G), an HNCO triple resonance spectrum (Muhandiram & Kay, 1994) was collected on a uniformly ^{15}N/^{13}C labeled sample. Although only seven peaks could be unambiguously compared with the same residue in Δ131Δ(WT) in 6 M urea (Wang & Shortle, 1995), the chemical shifts of the carbonyl carbons of K16, D19, M26, K28, M32, L36, and L38 were measured. In each case, the measured value in the L37G mutant was within 0.2 ppm or less of that of the Δ131Δ(WT) in 6 M urea, further supporting the conclusion that there is no significant persistence of extended structure in the β1, β2, β3, or h segments.

Hydrogen exchange kinetics of a closely related denatured state

Because the amide protons of the β1-β2-β3-h segment are absent from the ^{1}H-^{15}N correlation spectrum of Δ131Δ, the kinetics of hydrogen exchange cannot be measured directly by magnetization transfer (Mori et al., 1996). Residue-specific H_N assignments are available for the native state of staphylococcal nuclease (Torchia et al., 1989; Wang et al., 1992), and Δ131Δ can be refolded by addition of the tight binding ligands Ca^{2+} and 3′5′ thymidine bisphosphate (pdTp). However, preliminary experiments indicated that this stable, refolded state is not sufficiently long-lived to retain exchanged hydrogens for the hour or more required to collect a two-dimensional NMR spectrum in D_2O.

To study the hydrogen exchange kinetics of the β1-β2-β3-h segment in a denatured state that would permit stable refolding,

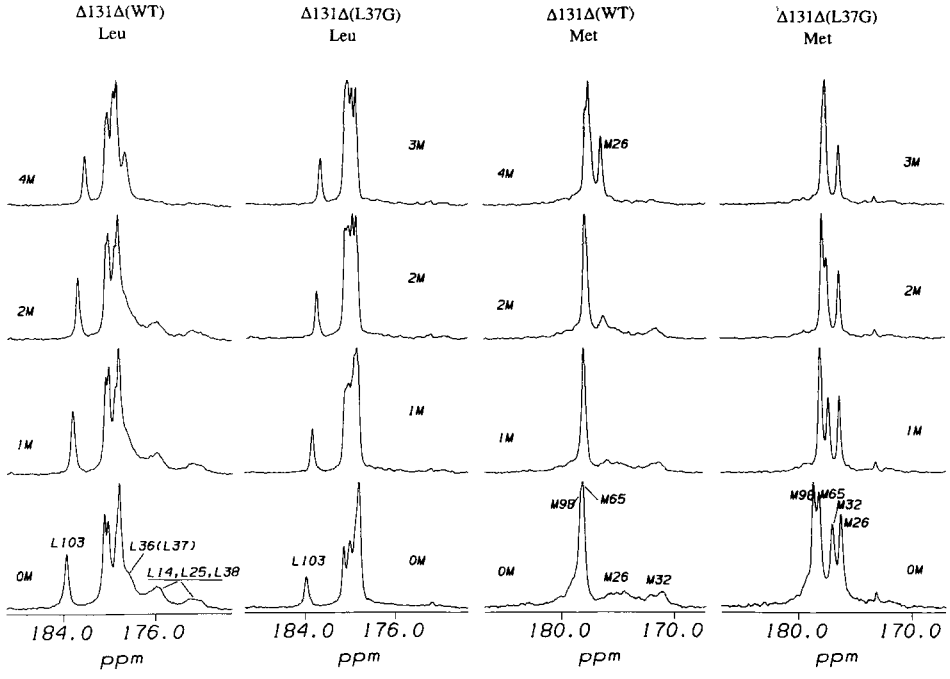

Fig. 5. ^{13}C-carbonyl spectra of Δ131Δ(WT) and Δ131Δ(L37G) labeled with either $^{13}C_1$-leucine or $^{13}C_1$-methionine, obtained at the urea concentrations marked on the spectrum.

experiments were performed on Δ135, a mutant of staphylococcal nuclease with the same amino terminal deletion as Δ131Δ but with an intact carboxy terminus (i.e, residues 1-3, 13 to 149). This mutant protein is approximately 4 kcal/mole more stable than Δ131Δ at 20 °C, pH 7.0 (Alexandrescu et al., 1994), and trial experiments demonstrated that, on binding Ca^{2+} and pdTp, it could retain its slowly exchanging amide protons for many hours in D_2O.

Hydrogen-deuterium exchange of the buried amide protons of Δ135 was quantitated at 20 °C, pH 4.3. Because at these solution conditions tryptophan fluorescence measurements indicated that Δ135 was 27% native and 73% denatured, exchange from the denatured state will be the only significant pathway for buried residues. ^{15}N-labeled Δ135 was deuterated by extensive exchange in D_2O, diluted into H_2O at time zero, and then exchange was stopped after varying time intervals by addition of Ca^{2+} and pdTp. After lyophilization, the refolded protein was dissolved in D_2O and a ^1H-^{15}N correlation spectrum was collected as rapidly as practical to quantitate the peak intensities of the slowly exchanging H_N in the folded state.

During the course of this work, it was noticed that Δ135 is significantly more stable in D_2O than in H_2O, being only 33% denatured at pD = 4.3 and 20 °C. However, when the temperature is raised to 43 °C, the fraction denatured is 70%, the same as under the conditions of exchange (80% H_2O, pH 4.3, 20 °C). Because the unfolding of Δ135 initiated by dilution from 100% D_2O to 20% D_2O is slower than hydrogen exchange, this shift in the denaturation equilibrium artifactually slows the apparent exchange rate to a common value for all residues. To avoid this artifact, exchange was initiated by rapid manual dilution of Δ135 in D_2O at 43 °C into H_2O cooled to 14 °C to achieve the desired conditions for exchange, namely 20 °C and 80% H_2O.

The kinetic curve for deuterium-to-proton exchange for six residues is shown in Figure 6, and the observed rates for the 30 unambiguously identified H_N peaks are listed in Table 1. Intrinsic exchange rates for fully solvent-exposed protons were calculated on the basis of the amino acid type of the residue detected and of the preceding residue (Bai et al., 1993); the ratio of this estimated intrinsic rate to the observed exchange rate defines the protection factor (Englander & Mayne, 1992). As can be seen in Table 1, except for residues in the second alpha helix (N100–G107), the protection factors were smaller than 6. For the nine protons in the β1-β2-β3-h segment, protection factors range from 0.8 to 3.2 and have values similar to those throughout the remainder of Δ131Δ. Because the uncertainty in the calculated intrinsic exchange rates can be as large as 2 to 3, these protection factors may not be significantly different from 1.0. Thus, these data suggest that structures involving hydrogen bonding between beta segments are only fractionally populated.

Characterization of a 44-amino acid fragment that includes β1-β2-β3-h

In an attempt to obtain more detailed structural information on the β1-β2-β3-h segment, a protein fragment that includes WT residues from 1 to 44 was generated by chemical cleavage (Stark, 1977) of the single cysteine mutant K45C. Although the efficiency of cleavage was typically only 80–90%, fragment 1–44 could be separated from the large fragment and uncleaved protein by FPLC cation exchange chromatography to greater than 97% purity. Because peptide bond cleavage at cysteine generates a free carboxy group plus an new, blocked amino terminus, fragment 1–44 does not contain any modified amino acids.

The far-UV CD spectrum of this fragment in Figure 7A reveals significant ellipticity between 210 and 230 nm in addition to the strong minimum at the random coil position of 200 nm. In 8 M urea, its spectrum closely approximates that of a random coil pep-

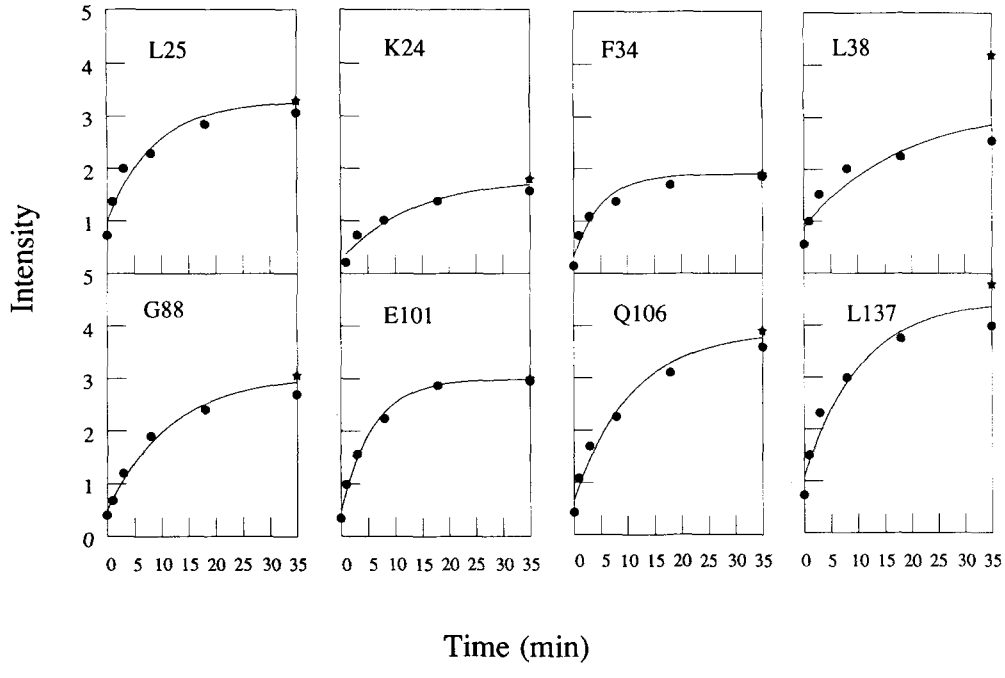

Fig. 6. Hydrogen exchange kinetics of eight representative amide hydrogens in Δ135, a more stable variant of the Δ131Δ fragment of staphylococcal nuclease, at pH 4.3, 20 °C. Peak intensity in arbitrary units from an HSQC spectrum is plotted as a function of time of exchange after shifting from 100% D_2O to 80% H_2O. The star at 35 min indicates the peak intensity after 4 h of exchange.

Table 1. *Hydrogen exchange rates at pH 4.3 and 20 °C*

Residue	k_{ex} (min^{-1})	Protection factor	H bonding in native 2° structure
V23	0.022	1.6	β2 → β3
K24	0.034	2.2	β2 → β1
L25	0.031	1.3	β2 → β3
Y27	0.049	1.6	
M32	0.034	1.9	β3 → β2
F34	0.048	2.2	β3 → β2
R35	0.049	3.2	
L38	0.019	1.0	
V39	0.019	0.8	
K64	0.050	2.8	α1
A69	0.064	3.7	
G86	0.023	4.0	Type I turn
G88	0.064	5.5	
L89	0.024	1.9	
A90	0.029	2.4	
Y93	0.027	1.3	β5 → β4
A94	0.038	3.4	Type I′ turn
V99	0.008	3.6	α2 → β5
N100	0.038	6.9	α2
E101	0.051	6.8	α2
V104	0.004	6.8	α2
Q106	0.046	4.7	α2
G107	0.052	6.5	Schellman motif
A109	0.028	2.5	
A112	0.034	2.5	
R126	0.036	2.3	α3
Q131	0.042	3.2	α3
K133	0.032	3.3	α3
K136	0.058	3.8	α3
L137	0.031	1.3	

tide. At longer wavelengths, the difference between 8 and 0 M urea spectra approximates the spectrum of the structure that is lost with the addition of urea, and, as shown in the inset, this difference spectrum has the pronounced minumum at 215 nm expected for beta sheet structure. A comparison of the CD spectra of Δ131Δ (Wang & Shortle, 1995) and 1–44 in the absence and presence of urea suggests that the β1-β2-β3-h structure can only account for approximately half of the beta sheet signal in Δ131Δ.

The one-dimensional proton NMR spectrum of fragment 1–44 in Figure 7B shows evidence for small amounts of stable, rigid structure. The upfield methyl group at 0.5 ppm, the downfield H_α at 5.5 ppm (plus several others just below 5.0 ppm), and the very broad envelope of H_N peaks around 9.0 ppm are not seen in Δ131Δ. Downfield-shifted H_α and H_N are considered to be diagnostic features of beta sheet structure. Unfortunately, the NMR spectrum changes slowly over several hours at 32 °C, with general broadening of peaks and disappearance of these three new spectral features, which presumably signals aggregation. Although preliminary experiments suggest that this problem may be less severe at lower temperatures and lower protein concentrations, it is not yet clear if conditions can be found that will permit a more detailed NMR analysis.

To characterize the state of aggregation of fragment 1–44 at a concentration of 0.5 mM, its diffusion coefficient was measured by a pulsed-field gradient-based NMR method (Altieri et al., 1995). The data (not shown) indicate the presence of a single major species with a diffusion coefficient essentially the same as that of WT native nuclease, which would correspond to a Stokes radius of approximately 15 Å. Although the sharpness of resonances in the aromatic and methyl regions suggest that the fragment is not aggregated extensively in solution, a Stokes radius of 15 Å could be consistent with either a dimeric species or a dynamic monomer with floppy amino and carboxy termini. If only the four hydro-

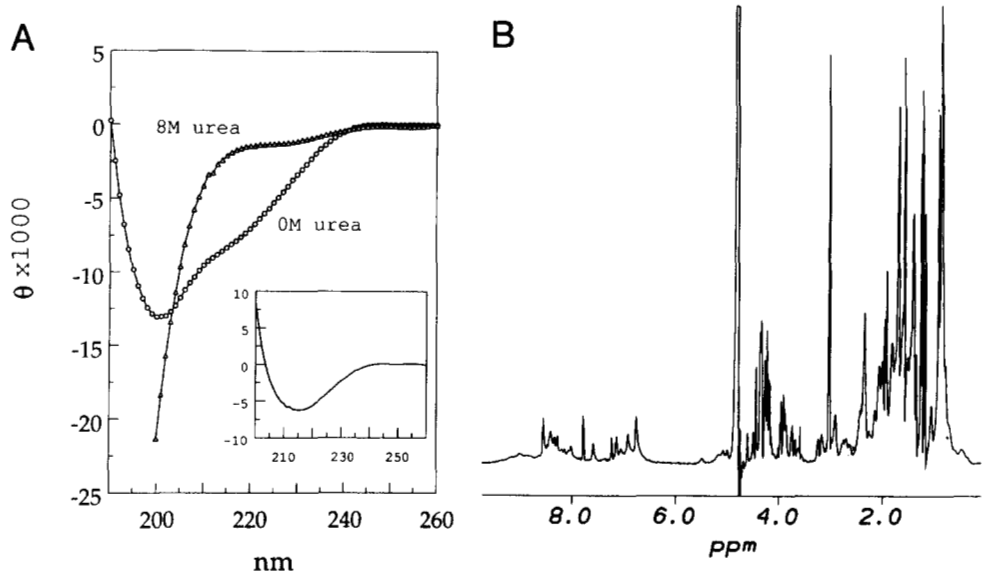

Fig. 7. A: CD spectrum of staphylococcal nuclease fragment 1–44 in either buffer pH 5.3, 32 °C, or in 8 M urea. Inset: Difference spectrum obtained by subtracting the 8 M urea spectrum from the spectrum in buffer. **B:** One-dimensional proton NMR spectrum of fragment 1–44 in H_2O, pH 5.3, at 32 °C, collected immediately after dissolution, 2.2 mM peptide, 32 transients.

phobic segments β1, β2, β3, and h participate in a compact structure, these termini are estimated to be 12 and 5 residues in length, respectively.

Discussion

These data clearly suggest that, in the denatured state, residues 13–39 of staphylococcal nuclease form a stable structure with extended, beta strand-like character. What makes this structure of particular interest is that it involves a combination of both native and non-native interactions. Whereas β1, β2, and β3 interact to form a three-strand antiparallel beta sheet (a beta meander) in the native conformation, the four large hydrophobic residues that follow β3—Leu 36, Leu 37, Leu 38, and Val 39—participate in a number of long-range tertiary contacts that do not include this beta meander. In the denatured state, however, they appear to fold back and form strong interactions with the three beta segments. When any one of these residues is mutated to glycine, altered behavior of this β1-β2-β3-h bundle is clearly reflected in both the ^{1}H-^{15}N correlation spectrum and the CD spectrum. By both methods, the rank order of mutant effects is the same: Leu 37 > Leu 38 > Leu 36 > Val 39.

The primary NMR criterion for formation of the this dynamic bundle is broadening of the amide proton resonances via intermediate conformational exchange. Mutations could cause these resonances to reappear simply by increasing the rate of exchange between the two or more conformations rather that by disruption of one (or more) conformations. In the case of the L37G mutant, the data suggest that the β1-β2-β3-h bundle has been disrupted. In addition to a sizeable reduction in the beta strand component of the CD spectrum, all of the missing amide protons are present in the ^{1}H-^{15}N correlation spectrum. On addition of urea, these peaks become somewhat sharper, but show no or only minor changes in ^{1}H and ^{15}N chemical shifts. If this structure were simply undergoing more rapid exchange between multiple conformations leading to chemical shift averaging, one would expect to see significant changes in chemical shift as the fractional population of the more random-like conformations increased at higher urea concentrations.

^{13}C NMR spectra of Δ131Δ with and without L37G support this same conclusion. The carbonyl resonances of V23, M26, M32, F34, V39, and several leucines in Δ131Δ(WT) respond to increasing urea concentrations by first shifting downfield in the direction of the random coil value and then sharpening. In the presence of L37G, these same resonances in the absence of urea are both shifted downfield and sharpened, and undergo only minor changes in chemical shift with increasing urea.

The disruption of the β1-β2-β3-h bundle by urea takes place gradually. The initial shifting of the $^{13}C'$ resonances to more random-coil values coincides with the dissociation of the β1 strand from the structure. Because the secondary shift of the ^{13}C carbonyl resonance is determined primarily by the backbone angle ψ, this observation suggests that the amplitude of the fluctuations in ψ may increase upon loss of β1. At still higher urea concentrations, the $^{13}C'$ resonances sharpen, suggesting that the rate of these large fluctuations increases, consistent with breakdown of the β2-β3-h bundle into free, random-coil–like segments.

We proposed initially that the β1-β2-β3-h structure consisted of a relatively stable beta meander with the hydrophobic segment from 36 to 39 covering the hydrophobic face of the three-strand sheet (Fig. 1). However, this model is no longer tenable in view of the fact that the protection factors of the five amide protons (Table 1) involved in strand pairing between these three beta strands are all less than 2. Instead, it would appear that this beta structure lacks the fixed hydrogen bonds associated with beta sheets. Hydrogen exchange kinetics of native WT nuclease support the conclusion that buried protons undergo exchange primarily through global denaturation, with the β1-β2-β3 segment exhibiting protection factors that are not significantly different from those of other elements of secondary structure (Loh et al., 1993). Nevertheless, the β1-β2-β3-h structure must be viewed as highly stable, because from 5 to 7 M urea is required to fully disrupt the interactions between β2, β3, and h.

Although the hydrogen exchange data rule out stable hydrogen bonds, the severe line broadening of the H_N, H_α, and C′ resonances suggests that there probably is not sufficient tight packing of atoms to permit stabilization of this structure by short-range van der Waals interactions. Thus, it would appear that hydrophobic interactions must provide the principle source of stability. A major role for hydrophobic interactions involving these segments is supported by the finding that glycine substitutions at V23 in β2, F34 in β3, and L36, L37, L38, and V39 in h all reduce the concentration of urea required for disruption of the structure.

Thus, the most reasonable structural model is that of a dynamic bundle of four adjacent chain segments, in which hydrophobic forces have acted to align the segments in a manner similar to that seen in liquid crystals (Fig. 8). Such a bundle (1) could form rapidly by a local zippering of neighboring residues, (2) would bury a significant amount of nonpolar surface, and (3) should still retain a relatively high entropy through sliding and bending motions.

Limited characterization of this chain segment in fragment 1–44 demonstrates that the β1-β2-β3-h bundle is stable in isolation from the remainder of the denatured state. Unfortunately, NMR spectroscopy of this fragment is complicated by the fact that it undergoes a slow change in state, presumably to form aggregates. One-dimensional proton spectra collected at lower concentrations soon after dissolution occasionally reveal several hallmarks of stable, well-packed structures: upfield methyl groups, and downfield alpha and amide protons. Although it is possible that structure in this isolated fragment is significantly different from the one formed in Δ131Δ, we consider it more likely that the two structures are the same, with the β1-β2-β3-h segment undergoing slower conformational exchange when removed from the rest of the molecule. Unlike the situation in intact Δ131Δ, there is no prospect in the fragment for subsequent folding interactions leading to the beta barrel and other structures in the short fragment. In the absence of the rearrangements of β1-β2-β3-h catalyzed by the presence of the rest of the protein chain, the rate of conformational exchange may be slow enough to permit NMR detection of some of the more structured conformations. Future studies of this and other fragments containing this chain segment may resolve this interesting issue.

A second, similar bundle formed from chain segments β4-β5-α2-β6* and apparently held together by hydrophobic interactions has been identified in Δ131Δ (Shortle et al., 1996; J. Gillespie & D. Shortle, unpubl. data). These findings raise the possibility that such partially native/partially non-native structures may be a general feature of compact denatured states. Such a scheme would be consistent with the general observation that proteins collapse rapidly to a compact state that subsequently undergoes much slower processes of rearrangement and structure fixation. Perhaps some of the general topologic features of proteins are determined by the number of such bundles, their relative strengths of segment–segment interactions, and the patterns of their fusion and rearrangement to form larger bundles in preparation for a liquid crystal-to-solid transition that forms rigid, well-packed native structure.

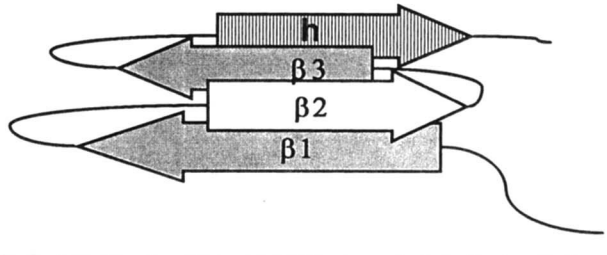

Fig. 8. A highly schematic model of the dynamic, beta-like bundle formed by the β1-β2-β3-h segment (residues 13–39) in the denatured state of staphylococcal nuclease. NMR data indicate that *this bundle is not a single structure*, as implied by the figure above, but rather a rapidly interconverting ensemble of many structures with this global topology.

Materials and methods

Protein samples

Samples of Δ131Δ, both as the "wild-type" sequence and six different single mutant forms, were prepared from a pET11 (T7) expression plasmid in a prototrophic strain of *Escherichia coli* according to previously published methods (Alexandrescu et al., 1994), using $^{15}NH_4Cl$ for uniform ^{15}N labeling, ^{13}C(6)-glucose for uniform ^{13}C labeling, and $^{13}C_1$-labeled amino acids for specific labeling. After extensive dialysis of column-purified protein against distilled/deionized H_2O and lyophilization, NMR samples were prepared in 10% D_2O and 1 mM sodium azide, with pH adjusted to 5.3 with 1 N HCl. In some cases, solid urea was added to a final concentration between 1 and 7 M, without further adjustment of the pH.

The 1–44 fragment was prepared from mutant protein K45C by thiocyanylation-alkaline cleavage according to the protocol of Stark (1977). Several milligrams of protein were dissolved in 1 mL of 6 M guanidine hydrochloride, 0.2 M Tris-HCl, pH 8.0. A threefold molar excess of dithiothreitol (DTT) was added and the mixture incubated for 40 min at 37 °C, at which point a 10× molar excess of NTCB to total thiol (DTT and K45C) was added. After 20 min at 37 °C, the thiocyanylation reaction was stopped by addition of 0.25 mL glacial acetic acid, and small molecules were removed by extensive dialysis of the protein against H_2O. Weak alkaline cleavage at sites of modified cysteines was obtained by dialysis against 100 mL 6 M guanidine hydrochloride in 0.1 M sodium borate, pH 9.0, at 37 °C for 18 h, followed by dialysis against H_2O. The efficiency of cleavage was approximately 80–85%. Fragment 1–44 was purified by chromatography in 6 M urea, 50 mM sodium formate, pH 3.1, on a Mono-S FPLC column using a shallow sodium chloride gradient. The purity of the final peptide was confirmed by electrophoresis on a urea/phosphate/SDS polyacrylamide gel.

NMR and CD spectroscopy

All NMR spectra were collected on a Varian UnityPLUS 600 MHz spectrometer using protein concentrations between 0.9 and 2.0 mM. ^1H-^{15}N correlation spectra were obtained with the sensitivity-enhanced HSQC pulse sequence of Kay et al. (1992) or the non-enhanced pulse sequence of Mori et al. (1995). Spectra of Δ131Δ, mutant forms of Δ131Δ, and fragment 1–44 were collected at 32 °C, pH 5.3, with the carrier frequency set on water (4.71 ppm) and a spectral width of 6,000 Hz using 512 complex points. In experiments involving an ^{15}N dimension, the spectral width was 1,300 Hz and the carrier set at 120 ppm. Typically, the ^1H dimension was apodized with a 15–30 degree shifted sine bell to enhance resolution, and the ^{15}N dimension with a 60–90 degree shifted sine bell, with the data size of both dimensions doubled by zero filling. Peak intensities were measured using the peak integration routine of FELIX 1.1. Parameters for the HNCO spectrum have been described previously (Wang & Shortle, 1995).

The ^{13}C carbonyl spectra of Δ131Δ with single phenylalanine, methionine, valine, isoleucine, and leucine labels were detected

directly at 150.8 MHz (carrier frequency 176.16 ppm) using a broad band probe by adding 2,048 transients of 608 complex points and a spectral width of 3,000 Hz. Each FID (free induction decay) was apodized with an exponential function (5 Hz broadening) and zero filled to 1,024 points.

CD spectra were obtained on an AVIV DS60 spectrometer, using a 0.1-mm-path length demountable cuvette thermostatted to 32 °C and protein samples with a final concentration of 1.2 mg/mL. Urea titrations were conducted on protein samples buffered to pH 5.3 with 20 mM sodium acetate. Each spectrum consists of five scans from 260 nm to 190 nm in 0.5 nm increments, which were added, smoothed, and corrected for the contribution of the buffer and cuvette.

Hydrogen exchange

Uniformly ^{15}N-labeled nuclease mutant Δ135 (residues 1–3, 13–145) was exchanged with D_2O by dissolving in 1.2 mL of D_2O followed by lyophilization, repeated twice. Exchange in 80% H_2O:20% D_2O was initiated by diluting 0.2 mL of protein (9 mg) in D_2O at 42 °C into 0.8 mL of H_2O at 14 °C. The final pH by glass electrode measurement was 4.3. The reaction mixture was incubated at 20 °C for 0, 1, 3, 8, 18, and 35 min or 4 h, and the reaction was stopped by adding Ca^{2+} and pdTp to final concentrations of 10 mM and 5 mM, respectively. After incubation on ice for 1 min, NaOH was added to a final pH of 6.3 to enhance Ca^{2+} and pdTp binding, and the sample was frozen and lyophilized. The amount of ^{1}H exchange for ^{2}H was quantified by dissolving the lyophilized sample in 0.6 mL of D_2O (0.9 mM final protein concentration). Within less than 60 min of dissolution, a high-resolution sensitivity-enhanced HSQC spectrum was completed (4 scans per real t_1 point, 128 complex t_1 points).

The natural logarithm of $I(4\text{ h})/[I(4\text{ h}) - 0.625 * I(t)]$, where $I(t)$ is the H_N peak intensity at time t, was plotted as a function of time and fit to the best linear least-squares line; this equation corrects for the 20% D_2O and gives the exchange rate in 100% H_2O (Connelly et al., 1993). This rate was multiplied by 1.33 to correct for the 25% of molecules that were native and therefore not undergoing exchange. The sequence-specific intrinsic exchange rate was calculated by the method of Bai et al. (1993), and the ratio of the calculated rate to the corrected observed rate gives the protection factor reported in Table 1.

Acknowledgments

We thank Tobin Sosnick for providing the program to calculate the dipeptide-specific intrinsic hydrogen exchange rates. This work was supported by a grant from the National Institutes of Health (GM34171).

References

Alexandrescu AT, Abeygunawardana C, Shortle D. 1994. Structure and dynamics of a denatured 131-residue fragment of staphylococcal nuclease: A heteronuclear NMR study. *Biochemistry 33*:1063–1072.

Alexandrescu AT, Shortle D. 1994. Backbone dynamics of a highly disordered 131-residue fragment of staphylococcal nuclease. *J Mol Biol 242*:527–546.

Altieri AS, Hinton DP, Byrd RA. 1995. Association of biomolecular systems via pulsed field gradient NMR self-diffusion measurements. *J Am Chem Soc 117*:7566–7567.

Bai Y, Milne JS, Mayne L, Englander SW. 1993. Primary structure effects on peptide group hydrogen exchange. *Proteins Struct Funct Genet 17*:75–86.

Connelly GP, Bai Y, Jeng MF, Englander SW. 1993. Isotope effects in peptide group hydrogen exchange. *Proteins Struct Funct Genet 17*:87–92.

Dill KA. 1985. Theory of the folding and stability of globular proteins. *Biochemistry 24*:1501–1509.

Englander SW, Mayne L. 1992. Protein folding studied using hydrogen-exchange labeling and two-dimensional NMR. *Annu Rev Biophys Biomol Struct 21*:243–265.

Kay LE, Keifer P, Saarinen T. 1992. Pure absorption gradient enhanced heteronuclear quantum correlation spectroscopy with improved sensitivity. *J Am Chem Soc 114*:10663–10665.

Loh SN, Prehoda KE, Wang J, Markley JL. 1993. Hydrogen exchange in unligated and ligated staphylococcal nuclease. *Biochemistry 32*:11022–11028.

Miranker AD, Dobson CM. 1996. Collapse and cooperativity in protein folding. *Curr Opin Struct Biol 6*:31–42.

Mori S, Abeygunawardana C, Johnson MO, van Zijl PCM. 1995. Improved sensitivity of HSQC spectra of exchanging protons at short interscan delays using a new fast HSQC (FHSQC) detection scheme that avoids water saturation. *J Magn Reson B 108*:94–98.

Mori S, Abeygunawardana C, van Zijl PCM, Berg JM. 1996. Water exchange filter with improved sensitivity (WEXII) to study solvent-exchangeable protons: Application to a zinc finger peptide. *J Magn Reson B*. Forthcoming.

Muhandiram DR, Kay LE. 1994. Gradient-enhanced triple-resonance three-dimensional NMR experiments with improved sensitivity. *J Magn Reson B 103*:203–216.

Shortle D. 1996. Structural analysis of non-native states of proteins by NMR methods. *Curr Opin Struct Biol 6*:24–30.

Shortle D, Wang Y, Gillespie J, Wrabl JO. 1996. Protein folding for realists: A timeless phenomenon. *Protein Sci 5*:991–1000.

Stark GR. 1977. Cleavage at cysteine after cyanylation. *Methods Enzymol 47*:129–132.

Torchia DA, Sparks SW, Bax A. 1989. Staphylococcal nuclease: Sequential assignment and solution structure. *Biochemistry 28*:5509–5524.

Wang J, Hinck AP, Loh SN, LeMaster DM, Markley JL. 1992. Solution studies of staphylococcal nuclease H124L. 2. ^{1}H, ^{13}C, and ^{15}N chemical shift assignments for the unligated enzyme and analysis of chemical shift changes that accompany formation of the nuclease-thymidine 3′,5′-bisphosphate-calcium ternary complex. *Biochemistry 31*:921–936.

Wang Y, Alexandrescu AT, Shortle D. 1995. Initial studies of the equilibrium folding pathway of staphylococcal nuclease. *Phil Trans R Soc Lond B 348*:27–34.

Wang Y, Shortle D. 1995. The equilibrium folding pathway of staphylococcal nuclease: Identification of the most stable chain–chain interactions by NMR and CD spectroscopy. *Biochemistry 34*:15895–15905.

Wishart DS, Sykes BD. 1994. Chemical shifts as a tool for structure determination. *Method Enzymol 239*:363–392.

Wishart DS, Sykes BD, Richards FM. 1991. Relationship between nuclear magnetic resonance chemical shift and protein secondary structure. *J Mol Biol 222*:311–333.